Sensitivity analysis for buckling characterisation using the vibration correlation technique

Baciu, Theodor D.; Degenhardt, Richard; Franzoni, Felipe; Gliszczynski, Adrian; Arbelo, Mariano A.; Castro, Saullo G.P.; Kalnins, Kaspars

DOI
10.1016/j.tws.2022.110329

Publication date
2023

Document Version
Final published version

Published in
Thin-Walled Structures

Thin-Walled Structures 183 (2023) 110329

Contents lists available at ScienceDirect

Thin-Walled Structures

journal homepage: www.elsevier.com/locate/tws

Full length article

Sensitivity analysis for buckling characterisation using the vibration correlation technique

Theodor D. Baciu [a,b,c,*], Richard Degenhardt [a,b,c], Felipe Franzoni [b], Adrian Gliszczynski [a,d], Mariano A. Arbelo [e], Saullo G.P. Castro [f], Kaspars Kalnins [g]

[a] Private University of Applied Sciences Göttingen, Composite Engineering Campus, Airbus Street No. 6, 218684, Stade, Germany
[b] DLR, Institute of Composite Structures and Adaptive Systems, Lilienthalplatz No. 7, 38108, Braunschweig, Germany
[c] University of Bremen, Fiber Institute Bremen eV Building IW3 Am Biological Garden 228359, Bremen, Germany
[d] Lodz University of Technology, Department of Strength of Materials, Stefanowskiego Street No. 1/15, 90-924, Lodz, Poland
[e] ITA, Aeronautics Institute of Technology, Department of Aeronautics, Praça Marechal Eduardo Gomes 50, Vila das Acácias, CEP: 12228-900, São José dos Campos, Brazil
[f] Aerospace Structures and Computational Mechanics, Faculty of Aerospace Engineering, Delft University of Technology, Kluyverweg Street No. 1, 2629 HS, Delft, The Netherlands
[g] RTU, Riga Technical University, Institute of Materials and Structures, Kipsalas Street No. 6b, LV-1048, Riga, Latvia

ARTICLE INFO

Keywords:
Vibration correlation technique
Sensitivity analysis
Shell buckling
Uncertainty quantification
Test set-up
Composite structures

ABSTRACT

The Vibration Correlation Technique (VCT) is a non-destructive method to predict buckling loads for imperfection-sensitive structures. While successfully used to validate numerical models and predict experimental buckling loads, recommendations for defining the VCT experiment are scarce. Here, its sensitivity towards the number of load steps and the maximum load level measured is studied, and an uncertainty quantification of the measured frequency affecting the VCT prediction is performed **First**, a series of finite element (FE) models representing nominally identical cylinders, and validated by buckling experiments, are used to perform a sensitivity study. When no frequency deviations are introduced in the FE results, a positive correlation between the VCT predictions and the maximum load used for measurements is found, the number of load steps used being only relevant in reducing the errors. Introducing frequency deviations deterred the predictions correlation with the maximum load, while using more load steps reduced this influence. **Second**, a sensitivity study based on experimental data confirmed most of the trends previously observed using the FE results, the exception being a poor prediction sensitivity as a function of the maximum load, owing to several cylinders for which the VCT method gave predictions that progressively decreased with increasing the load.

1. Introduction

Buckling is one of, if not the most, important sizing criteria for cylindrical shells, especially for launcher structures. This, combined with the inherent high buckling load sensitivity of these structures to imperfections and the potentially destructive nature of this phenomenon led to an ever-increasing interest of non-destructive experimental method to predict it. These are typically based on extrapolating the instability point from their response at load levels below the buckling load. Among the most established ones are the VCT [1], based on the change of the vibration response with increasing the load, the probing technique, based on laterally probing the cylindrical shell and tracking its load–displacement response under different cylinder load levels [2–4], or the Southwell plot [5,6], which is based on tracking the lateral deflections to predict the instability point.

Since the discovery of the influence of applied loads over a structure's vibration response, one of the main uses of this relation was for predicting the buckling loads of different structures. Predicting a structure's buckling load using the change in its vibration response with the applied load is now commonly referred to as the VCT. Besides the aforementioned application, another common use of VCT is in the determination of in-situ boundary conditions. In the present work, VCT is used in the first context, namely to predict buckling loads.

Throughout the years, VCT approaches were applied and developed for structures like beams and columns [7,8], plates [9], stiffened plates [10,11], cylindrical shells [12], or stiffened cylindrical shells [13] to name a few. VCT is particularly attractive for unstiffened shell structures, given their unstable buckling, their high sensitivity to imperfections, and the non-destructive nature of the method. One

* Corresponding author at: DLR, Institute of Composite Structures and Adaptive Systems, Lilienthalplatz No. 7, 38108, Braunschweig, Germany.
E-mail addresses: theodor.baciu@dlr.de (T.D. Baciu), Richard.Degenhardt@dlr.de (R. Degenhardt), Felipe.Franzoni@dlr.de (F. Franzoni), adrian.gliszczynski@p.lodz.pl (A. Gliszczynski), marbelo@ita.br (M.A. Arbelo), S.G.P.Castro@tudelft.nl (S.G.P. Castro), kaspars.kalnins@latnet.lv (K. Kalnins).

https://doi.org/10.1016/j.tws.2022.110329
Received 6 June 2022; Received in revised form 26 August 2022; Accepted 31 October 2022
Available online xxxx
0263-8231/

common application for unstiffened shells is in space structures, for which reliable buckling load predictions are of paramount importance. VCT has the potential to both replace the, potentially destructive, buckling experiment of shells, providing a reliable, non-destructive method to accurately predict buckling loads and to assess the buckling load degradation of reusable space structures. Although multiple promising results are readily available in the literature regarding the method's accuracy in predicting buckling loads, the application of VCT for cylindrical shells is still under development [14].

Some of the earliest examples of VCT come from Sommerfeld [7] and Melan [8], who studied the relation between a beam's vibration response and its loading at the beginning of the 20th century. For these types of structures, the buckling and vibration modes are identical for simply supported boundary conditions, giving a linear relation between the applied compressive load P and the square natural frequency F_k:

$$f_k^2 + p = 1 \tag{1}$$

where, p is P/P_{cr}, P_{cr} is the linear buckling load, f_k is $F_k/F_{0,k}$, $F_{0,k}$ is the kth natural frequency in the unloaded/reference state, and F_k is the kth natural frequency at a load level P. The experimental procedure consists in plotting f_k^2 against P and then to extrapolate using a linear fit the value of P for which $f_k^2 = 0$. While the method was experimentally validated in the first decade of the 20th century [7], other experimental campaigns were only carried out in the 1950s [9,10].

The relationship for beams and columns has little sensitivity to boundary conditions (small deviations from a linear relation), rendering the method applicable for boundary conditions other than simply supported [9,15,16]. This relation can also be extended to plates and shells, but its applicability is restrained mainly to imperfection insensitive structures and to structures with negligible imperfections [9,11, 16].

In [17], Souza et al. proposed a novel VCT approach for columns and shells, based on a modified characteristic chart in which the following linear relationship between $(1-p)^2$ and $1-f_k^4$ is used [18]:

$$(1-p)^2 + (1-\xi_k^2)(1-f_k^4) = 1 \tag{2}$$

where ξ_k^2 represents the drop of the buckling load due to initial imperfections. The buckling load is found by linearly extrapolating for $(1-p)^2 = \xi_k^2$ at $(1-f_k^4) = 1$, and the value of ξ_k^2 should be positive for it to have a physical meaning.

Arbelo et al. [19] proposed an empirical relation, at that time, in which instead of plotting $(1-p)^2$ against $1-f_k^4$, $(1-p)^2$ was plotted against $1-f_k^2$. This relationship between the load and natural frequency is represented by a second order fit, in which the minimum value of $(1-p)^2$ represents the square of the drop of load carrying capacity ${\xi_k}^2$. Using this relation, the buckling load prediction can be obtained using Eq. (3) [19]:

$$P_{VCT,k} = P_{cr}(1 - \sqrt{{\xi_k}^2}) \tag{3}$$

This relation was later analytically verified by Franzoni et al. in [20] for simply supported shells under compression, in which the following relation was obtained:

$$(1-p)^2 = [1-(1-f_k^2)]^2 \tag{4}$$

showing analytically that indeed there is a second order relation between $(1-p)^2$ and $1-f_k^2$, as proposed by Arbelo in [19]. This approach was also experimentally validated in multiple campaigns [19–32]. A thorough review on the VCT methods for different types of structures was also provided by Abramovich in [14].

The rising interest for using the VCT for bucking characterisation led to multiple sensitivity analyses of the method to: boundary conditions, shape and thickness imperfections, combined loading, or cut-outs. Souza showed the sensitivity of the natural vibration frequencies to the shape of initial imperfections in [33] and to the boundary conditions in [34]. In his studies, he found that the natural vibration frequencies of beams and plates tend to increase with the magnitude of their imperfections, while for shells the opposite occurs. Furthermore, Souza also showed that the vibration response of shells greatly differs between simply supported and clamped boundary conditions. In the work of Arbelo et al. the importance of including the appropriate material properties, boundary conditions, shape imperfections and thickness imperfections in numerical simulations for reliable VCT buckling load predictions was shown [19,24,35].

Skukis et al. in [21,25] showed that VCT is also applicable for cylinders with cut-outs, given that the shell would experience a global, rather than a local, buckling. The presence of large cut-outs can create a local out-of-plane deflection that acts as a local instability initiator [22], rendering the VCT unfeasible. However, this aspect can be alleviated if the cut-out is reinforced, such that the cylinder buckles globally [21]. Furthermore, Skukis et al. also emphasised the influence of including shape imperfections, in-situ boundary conditions, and the test rig elements in their simulations for accurate VCT predictions. The influence of internal pressure was also studied in the work of Franzoni et al. [20,23], who showed that VCT is also applicable to stiffened pressurised cylindrical shells. Regarding truncated conical shells, Gliszczyński et al. [36] investigated the predictive capabilities of VCT for types of structures, using the FE models of two composite cones of nominally identical geometry, but with different ply topology. An extensive parametric study, considering different bottom radii, semi-vertex angles, length, plus initial thickness and shape imperfections, was also performed. The authors highlighted the conservativeness of the method for the studied structures, found that the VCT predictions are more sensitive to the initial shape imperfection and ply topology when compared to the overall compressive response, that VCT is relatively insensitive to thickness imperfections and that higher load ratios provided better accuracy.

One of the first estimations of the influence of the frequency measurement errors over the VCT predictions was given by Segall and Springer in [37]. In their study for flat plates, the inspection of the equations used revealed that any error in the frequency measurement would double its effect in the VCT predictions. The monotonicity between the measurement errors and the VCT predictions errors was also observed by Go et al. [38] for beams, where experimental measurement errors from 2% to 6% turned into buckling load prediction errors from 5% to 20%, depending on the beam's boundary conditions.

Two particular aspects that can influence the method's accuracy are the maximum load level measured and the number of load steps used for the VCT predictions. Furthermore, these aspects are also important when preparing an experimental test, as the number of load steps could be restricted due to time constraints, while the maximum load could be restricted due to the risk of damaging the tested structure, or due to the confidence in the predicted buckling load. The maximum load level needed for reliable VCT predictions in particular appears to be highly dependent on the experiment and structure, with high variations for accurate VCT predictions being reported. In the work of Arbelo et al. [24], load levels from 50% of the experimental buckling load and above were needed for satisfactory VCT predictions, while in the work of Kalnins et al. [26], satisfactory predictions were obtained only when using compressive loads above 85% of the experimental buckling load. The literature reports on the number of load steps needed for a reliable VCT prediction are also scarce, this number varying from 6 in the study of Franzoni et al. [27], to at least 15 in the work of Labans et al. [28], 15 measurements being also the recommended number of load steps in [24].

In the present paper, the authors advanced their previous work [39], by including experimental data and extending the numerical one, in a sensitivity study on the evolution of the VCT buckling load predictions as a function of the load level and the number of load steps measured, including the influence of frequency measurement deviations. The study aims to observe trends in the VCT buckling load predictions as a function of the aforementioned factors, trends that can be used to efficiently design a robust test plan for applying VCT to cylindrical shells.

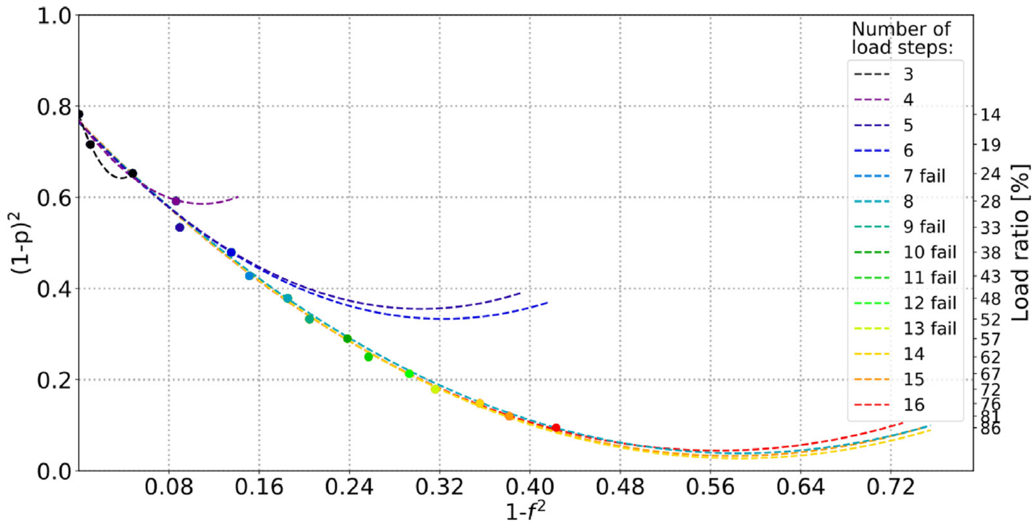

Fig. 1. Quadratic curve fits for the first vibration mode with increasing the number of load steps [28].

2. Methodology

The VCT method used here is the Arbelo's approach [19], in which the analytical relation between the structure's natural frequency and the compression load applied is shown in Eq. (4) [20]. For a valid prediction, $\xi_k{}^2$ from Eq. (3) must be higher than 0 (the linear buckling load being found for $\xi_k{}^2 \sim 0$), the 'x' coordinate of the minimum must be larger than the one of the last measurement and the minimum number of load steps required is 3, as the number of load steps needs to be higher than the order of the fit.

One example of the VCT application is shown in Fig. 1, where the experimental VCT data of a composite cylinder with a variable angle tow was taken from the available literature [28] and used to perform quadratic fits, starting from the minimum number of load steps, and progressively adding all the load steps available. In this case, there were 16 measurements used, at the load ratios shown on the secondary *y*-axis of the figure, the last one being at a load ratio of 86% from the cylinder's experimental buckling load.

From this figure, important observations laying the foundations of this work can be drawn. First, one can notice that not all the points follow closely a quadratic curve and also that in some cases a valid quadratic curve cannot be fitted through the points. There are several reasons why this can happen, like small load variations during the measurement, measurement errors, small changes in the load path at small load levels, or local phenomena at higher load levels (buckling; damage).

Furthermore, particularly when using a low number of load steps with large deviations, the quadratic fit could even give a maximum, instead of a minimum point, rendering the fit unusable for VCT buckling load predictions. In the given example one of the most obvious deviations happened between the points corresponding to the load steps at a load ratio of ~28% and ~33% respectively, where the difference between the frequencies was small compared to the other load steps. Having two load steps with a small frequency difference between them, when compared to the other measurements, can not only yield unreliable predictions, but also interfere with the curve fitting process altogether. Therefore, for the extreme cases where most of the quadratic fits failed due to these types of deviations, one of the two frequency measurements was discarded. The decision on which of the two measurements should be kept was taken based on the improvement given by keeping that measurement, namely by the number of the additional intermediate valid VCT predictions provided.

Furthermore, when comparing the load ratios from Table 1, showing the first and last measurements performed for this cylinder, with the ones from Fig. 1, one can notice that the first few measurements were

Table 1
Load steps with corresponding load ratios and vibration frequencies for the first mode [28].

Load [kN]	Load ratio [%]	Vibration modes frequencies [Hz]
10	4.8	226.2
20	9.6	231.0
30	14.4	231.2
40	19.2	230.0
50	24.0	225.6
…	…	…
160	76.9	185.6
170	81.7	181.8
180	86.5	175.6

not used for the VCT prediction. In this case, it can be seen by inspecting the first 3 measured frequencies that these were initially increasing, while a decrease was expected given the increase in the compressive load. This likely happened since, for these low load levels, there were still some settling events, with the boundary conditions and load path slightly changing as firm contact was ensured within the test machine and between the load introduction surfaces and the tested structure. Such measurements were also removed for the other experimental data sets where it was observed that initially the frequencies increased with increasing compressive load.

Fig. 1 also shows that the minimum $\xi_k{}^2$ of the curves generally decreases with increasing the number of load steps/maximum load ratio used. This translates into a VCT buckling load prediction increase, generally quasi-linear, as a function of the same parameters. Also, this increase often gives more accurate VCT predictions, given the generally conservative nature of the method. However, in this figure there is a direct coupling between the number of load steps and the maximum load ratio (since they were increased simultaneously and each measurement corresponds to a certain load ratio), meaning that here the sensitivity of the VCT predictions to each of these parameters cannot be assessed independently. In order to study the influence of these two parameters over the VCT predictions independently, more VCT predictions must be generated, such that these predictions can be classified separately as a function of the number of load steps and the maximum load ratio used. The method chosen here was to use the available data to generate combinations of r load steps out of total number of measured load steps n using the combinations formula:

$$C(n, r) = \frac{n!}{(n, r)!r!}, r = 3, 4 \ldots n - 1 \quad (5)$$

and then to perform a VCT prediction for each load steps combination. This approach does not entirely decouple the influence of the two parameters, as the lower bound of the maximum load ratio increases with the number of load steps used. For example, at the lowest spectrum ($r = 3$), the maximum load ratio would be equal to, or higher than, the one of the 3rd load step, while for any other r, the maximum load ratio would be equal to, or higher than, the one of the rth measurement. When put in numbers, for $n = 10$ load steps with the last two measured load steps at 80% and 85% load ratios, for any combination with $r = 9$, the maximum load ratio will automatically be either 80%, or 85%. Regardless of the residual coupling between the number of load steps and the maximum load ratio, using this approach to generate combinations of load steps using the combinations formula (5) and to evaluate each of them using Eq. (3) allows a more detailed analysis over the influence of the number of load steps and maximum load ratio on the VCT buckling load predictions.

The influence of measurement deviations on the VCT predictions was already shown in Fig. 1. Given the possibility to accurately control the load during an experiment, here the sensitivity of the used VCT method to measurement deviations was chosen to be studied by altering the natural frequencies. To the authors' best knowledge, there is limited information regarding the expected frequency measurement deviations. In the work of Franzoni et al. [23], the authors compared the frequency measurements between two equipment monitoring the vibration response of the same structure at different locations. Out of a total of 12 load steps measured, the frequency difference between the two equipment was 0 Hz for 9 load steps, 0.25 Hz for 2 load steps, and 1.5 Hz for 1 load step. The fact that most of the measurements given by the two equipment appeared identical, and the 0.25 Hz measurement resolution used, suggest that most often the measurement deviations are below 0.25 Hz, with higher, more isolated, deviations being also possible. As the information on expected frequency deviations is scarce, for the sensitivity studies here three maximum allowed frequency deviation magnitudes were chosen. These are ±0.1 Hz, ±0.25 Hz and ±0.5 Hz. For each of these maximum frequency deviations, 50 altered data sets were generated for each VCT data set to avoid the influence of possible outliers given by certain particularly unfavourable combinations of load steps. These altered data sets were generated from the nominal numerical/experimental results, by applying random deviations within the aforementioned limits to each frequency of the load steps considered. After these altered data sets were generated, the same approach of generating load steps combinations using the combinations formula (5) was used, generating a VCT buckling load prediction using Eq. (3) for each load steps combination. Also, since the accuracy of the method itself is not of interest in this study, for an easier visualisation of the results all the VCT predictions were normalised with respect to the nominal VCT prediction (obtained using all the load steps of that respective data set).

3. Sensitivity study based on FE results

The main purpose of the numerical study is to provide an underlying foundation for the study using experimental data, as well as to better assess the influence of the frequency measurement deviations on the VCT buckling load predictions, given that such deviations would always be present in the experimental data. The numerical models used in this study were defined for a family of nominally identical, unstiffened, CFRP cylindrical shells, shown also in the work of Degenhardt et al. [40]. The actual cylinders used were Z15, Z17, Z18, and Z20–Z26 and for which VCT results were shown in [19,41]. The cylinder's layup is [±24, ±41], with a thickness of 0.5 mm, a total length of 540 mm, a free length of 500 mm (between the potted ends), and a radius of 250 mm (nominal dimensions). The material properties for the nominal ply, Hexcel IM7/8552, are shown in Table 2. The material properties of the potting used at the ends for a uniform load introduction are: E = 2.45 GPa, $\nu_{12} = 0.3$, and $\rho = 2090$ kg/m^3.

Table 2
Hexcel IM7/8552 CFRP ply material properties [41].

E_1 [GPa]	E_2 [GPa]	G_{12} [GPa]	ν_{12}	ρ [kg/m^3]
142.5	8.7	5.1	0.28	1580

The numerical analyses were conducted using the ABAQUS finite element software and had the measured dimensions, shapes and thicknesses imperfections of the cylinders implemented using the approach described and validated in [42], thickness and shape imperfections reported in detail in [36]. In this approach, the material properties of the elements are also altered to account for the measured thicknesses. The CFRP cylinder is modelled with S8R shell elements, while the potting is modelled with C3D20R brick elements. A more detailed description on the FE models used can be found in [41].

3.1. Results

The linear buckling loads P_{cr}, between 30.25 kN and 33.02 kN, were determined using the FE models by means of a buckling eigenvalue analysis. These models were built considering the measured dimensions and considering the average thickness to alter the material properties using the rule of mixtures. The non-linear buckling loads of the models, between 20.32 kN and 26.83 kN, were obtained by running static general analyses, assuming geometric non-linearities, as well as the measured thickness and shape imperfections, according to the methodology described in [42]. The natural frequencies were extracted using the latter models, in load steps of a 5% load ratio with respect to their non-linear buckling loads. Therefore, the natural frequencies were obtained for 20 load steps, from a 0% load ratio, up to a 95% load ratio. These values were used, together with their corresponding load levels and linear buckling loads to give VCT buckling load predictions. This approach considering a high number of load steps and extreme load ratios was chosen in order to allow a more in-detail preliminary analysis, which otherwise would be difficult to perform experimentally. However, such a numerical analysis including several FE models can be not only computationally heavy, but more importantly, also not necessarily relevant for a realistic VCT test. One of the possibly unrealistic scenarios is measuring such a large number of load steps. Given the typically frequency response measuring method [23,24,26–28] and depending on the combination of the measurement detail and the number of load steps measured, the holding time needed for a single measurement can lead to a prohibitive total testing time. Furthermore, measuring at high load ratios comes with high risks of catastrophic buckling occurring during the measurement, in which the load should be kept constant. Last, using this approach gives some predictions using load steps at load ratios which can be irrelevant for a real test. For example, predictions using low maximum load ratios would be included, which is counterintuitive when considering that the accuracy of the used VCT approach tends to increase with the maximum load level measured. In order to address the aforementioned points, several load criteria were implemented, such that only more realistic load steps combinations were used to perform the numerical VCT buckling load predictions. These load criteria used to filter the VCT predictions are:

1. Maximum load ratio in the 50%–85% interval
2. Bias towards higher load levels
3. Minimum load ratio within 15%
4. Maximum load ratio gap of 20%

The lower limit of the first criterion was chosen such that predictions using points on the quasi-linear region of the characteristic chart only were avoided and due to accuracy concerns. Given that FE models can robustly predict buckling when imperfections are accounted for (boundary conditions, loading, shape, thickness) and that VCT can also be used in-situ to give buckling load predictions, the higher limit at

85% was chosen as it was considered to be a safe limit for VCT testing. The second criterion ensures that in a given load steps combination, most of the load steps are above the middle of that specific load steps combination. For example, while a load steps combination such as [10%, 25%, 40%, 50%] will go through, as more than half of the entries are above (50–10)/2%, a load steps combination such as [10%, 25%, 35%, 85%] will not go through, as most of the entries are at lower load ratios than (85–10)/2%. The minimum load ratio of 15% was chosen such that the change of the frequency response of the structure with applied load would be considered in this region as well. This criterion was implemented as it was observed that, when failing to do so, the quadratic fit can miss the points corresponding to low load ratios by a large amount, describing thus an unrealistic behaviour. The last criterion was adopted such that high load ratio discrepancies between consecutive load steps are avoided and that the quadratic fit is performed using points relatively evenly distributed between the extremes. An example of a combination of load steps that would be avoided is [5%, 75, 80%, 85%], as missing the points corresponding to intermediate load ratios might introduce large deviations with respect to the fit when using all the points.

3.2. Sensitivity study

Fig. 2 shows in violin plots the predictions for the first vibration mode, with and without the load steps criteria applied. Here the predictions without load criteria are shown in orange, while the predictions satisfying the load criteria are shown in blue, representing roughly 7% out of the entire data. In these violin plots, the top and bottom horizontal lines show the extreme predictions, the lines in between the top and bottom ones show the medians of the distributions, while symmetrically across the vertical lines the distribution shapes of the VCT predictions can be seen. Besides the number of load steps on the bottom horizontal axis, there is also a secondary top horizontal axis, which shows the number of the VCT predictions contained in each violin plot without load criteria applied and in percentages the number of predictions with load criteria applied out of the ones without load criteria applied. This secondary horizontal axis at the top also shows the data distribution with respect to the number of load steps. In this case, for the unfiltered data the distribution can be considered quasi-normal, as the number of the VCT predictions is quasi-symmetric about the violin plot corresponding to 10 load steps used (half of the maximum number of load steps), due to the nature of the combination's formula (5). However, due to the load criteria applied, for the filtered predictions the distribution is no longer quasi-symmetric.

When looking at Fig. 2, one can notice several trends. First would be that the amplitude of the predictions tends to decrease with increasing the number of load steps, especially for the unfiltered predictions. This is due to the fact that for a low number of load steps, there can be many combinations for multiple maximum load ratios, while when approaching the maximum number of load steps, the possible maximum load ratios become more restricted. Also, the median initially increases with the number of load steps and when more than 5–6 load steps for the unfiltered data, or more than 8–9 load steps for the filtered data, are used for the predictions, it tends to stabilise to a constant value of 1. This aspect is better seen for the filtered data where, due to the load criteria, the number of combinations containing high load ratios is scarce for a low number of load steps. This is also the reason why for a low number of load steps most of the filtered predictions are relatively far from the predictions using a larger number of load steps. When increasing the number of load steps used, the predictions also tend to form 'clusters', with the main one tending to align with the prediction obtained using all the load steps. These clusters are defined here as the areas in the VCT predictions distributions between consecutive positive inflection points, or between areas where the width of the distribution is approximately 0. The predictions from different maximum load ratios, or cylinders, can create such clusters, which can also overlap, giving a wavy appearance to the distributions. Regardless of the large VCT predictions amplitudes of these clusters when compared to the amplitudes including the extremes, the maximum amplitudes are still extremely low, at ~0.1. This occurred due to the numerical nature of these results, where the minimum $\xi_k{}^2$ of the characteristic curves varied little, regardless of the cylinder and maximum load ratio, as all the points followed closely a quadratic behaviour. This type of behaviour is ideal when using VCT, as it means that the buckling load prediction varies little with both the number of load steps and the maximum load level considered, allowing robust predictions using safe load levels.

Perhaps one of the major differences between the filtered and unfiltered data is seen for a lower number of load steps. Here the extreme predictions for the unfiltered data were obtained using the minimum number of load steps (3), while for the filtered data these were seen between 6–11 load steps.

For the assessment of the influence of the maximum load ratio parameter over the VCT buckling load predictions, another figure with violin plots was created. Fig. 3 shows the predictions from Fig. 2, rearranged such that now there is a violin plot for each maximum load ratio interval used. While the FE results were taken at explicit load ratios, the results are shown here as a function of load ratios intervals, for a better consistency with the results based on the experimental data, since measuring at pre-defined load ratios is difficult. For clarity, the intervals defined have a (m, n] form, meaning that in this case the (60–65]% interval would contain only the results from a 65% load ratio. Here it can be seen that there is definitely a monotonic relation between the VCT predictions and the maximum load ratio, for both the filtered and unfiltered data. Also, some small clusters can be seen at the top of several violin plots, these being likely given by the VCT predictions of a specific cylinder. Furthermore, the range of the predictions seems to decrease with increasing the load ratio, despite the ever-increasing number of VCT predictions with the load ratio. This suggests that using load steps at higher load ratios could also reduce the variations given by the combinations of load steps at lower load ratios.

When looking at Figs. 2 and 3 and upon inspecting the extreme predictions of the unfiltered predictions, it can be seen that generally the lowest VCT predictions are obtained using the lowest number of load steps, at the lowest load ratios, while the highest predictions are found when using 3–4 load steps, but this time all at load ratios in the [85–95]% interval. When the load criteria are applied, the maximum amplitude and the lowest predictions are no longer found when using a low number of load steps, as the extreme predictions using load steps exclusively at low/high load ratio are filtered out. The largest predictions amplitudes with respect to the number of load steps used is no longer found at the extremes, while the predictions with respect to the maximum load ratio used follow the same behaviour as for the case with unfiltered load steps.

Overall, this study suggests that the lowest VCT predictions would be found using few load steps at extremely low load ratios, while the highest ones would be found using also few load steps, but at very high load ratios.

Furthermore, it also suggests that the number of load steps has little influence over the VCT predictions, while the VCT predictions seem to highly depend on the maximum load ratio.

The correlations of the number of load steps and the maximum load ratio used with the VCT predictions can be further studied using established statistical tools to quantify the influence of these two parameters. Correlation coefficients such as Pearson's r, Kendall's τ, or Spearman's ρ can be of particular interest, as they can identify the strength of the linear relation between two variables, the strength of their dependence, or their strength of association [43–45]. While using a Pearson r correlation coefficient to classify the degree of linearity between the maximum load ratio, or the number of load steps, and the VCT predictions would be of high interest, unfortunately the required assumptions of this correlation coefficient cannot be satisfied. The

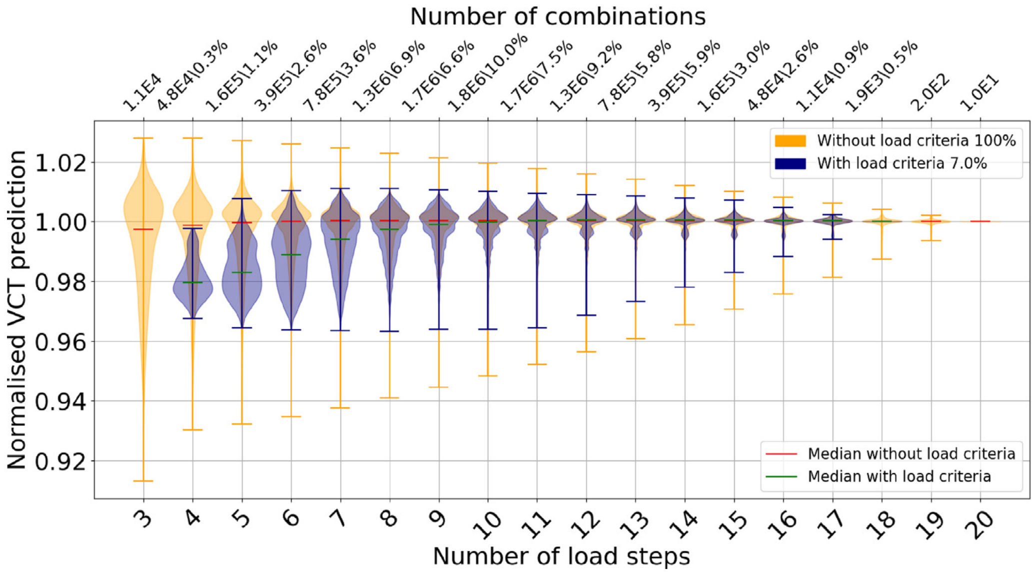

Fig. 2. VCT predictions as a function of the number of load steps, pristine numerical data.

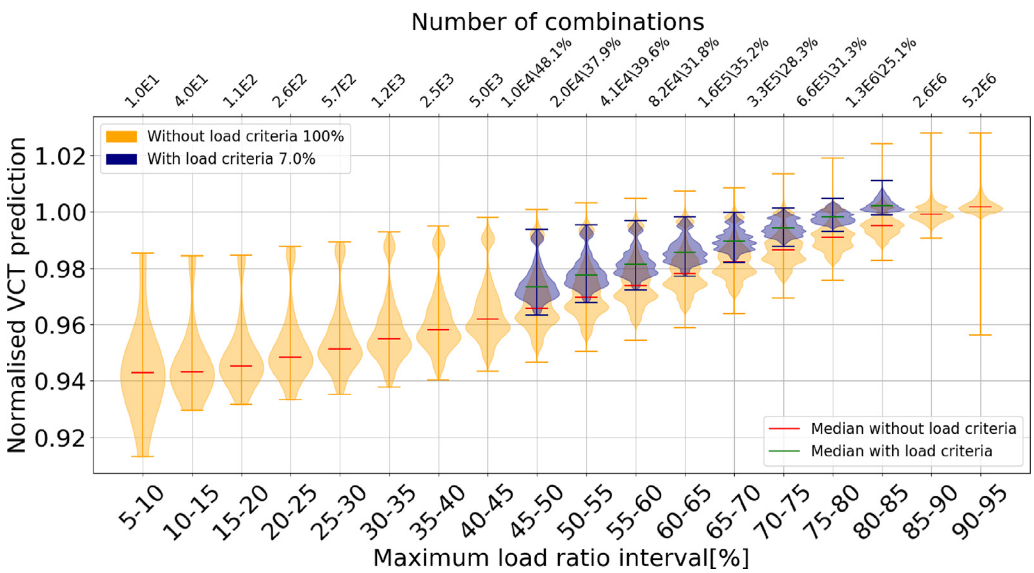

Fig. 3. VCT predictions as a function of the maximum load ratio, pristine numerical data.

VCT predictions classified as a function of the maximum load ratio fails the need of normally distributed data (increasing VCT prediction counts on the top horizontal axis of Fig. 3), while the predictions classified as a function of the number of load steps are intrinsically not continuous. Furthermore, outliers can reduce the relevance of this correlation coefficient, an aspect valid also for Spearman's ρ correlation coefficient, although to a far lesser extent. On the other hand, Kendall's τ is relatively insensitive to outliers, the analysed data has to be at least ordinal, if not continuous, and it is generally more robust than the Spearman's ρ. Therefore, for our VCT predictions, the Kendall's τ appears to be the best option of the three to study the correlations between the two parameters of interest and the VCT buckling load predictions. The correlation coefficient can range from −1 to 1, showing the strength of the monotonic relation between each two variables compared, with $\tau - 1$ for a monotonic decrease, 1 for a monotonic increase, while a coefficient of 0 shows the absence of a monotonic relation between the two variables. In terms of effect size, there is no general agreement on what magnitude of this coefficient shows a weak, moderate, or a strong correlation [46,47]. For this study, the following effect size is considered for the correlation coefficients: 0.07–0.21 shows a week correlation, 0.21–0.35 shows a moderate correlation and anything above 0.35 shows a strong correlation [47].

Fig. 4 shows a heatmap of the Kendall correlation coefficients for the analysed data. In this figure, the numbers inside the boxes represent the correlation coefficients between the variables corresponding to the line and column on which it is located.

When looking at the correlation coefficient between the number of load steps and the maximum load ratio for the unfiltered predictions, one can see that $\tau = 0.22$, which indicates a weak-to-moderate correlation between these two parameters. This weak-to-moderate correlation is expected, given that these parameters are not fully decoupled. This correlation for the filtered load steps becomes moderate, with $\tau = 0.33$, as the applied load steps criteria favours higher maximum load ratios. Furthermore, the correlation between the number of load steps and the VCT buckling load predictions is absent for the unfiltered data ($\tau = 0$) and weak for the filtered data ($\tau = 0.13$). This confirms the absence of a monotonic relation between the VCT buckling load predictions and the number of load steps used to generate them, as for the filtered data

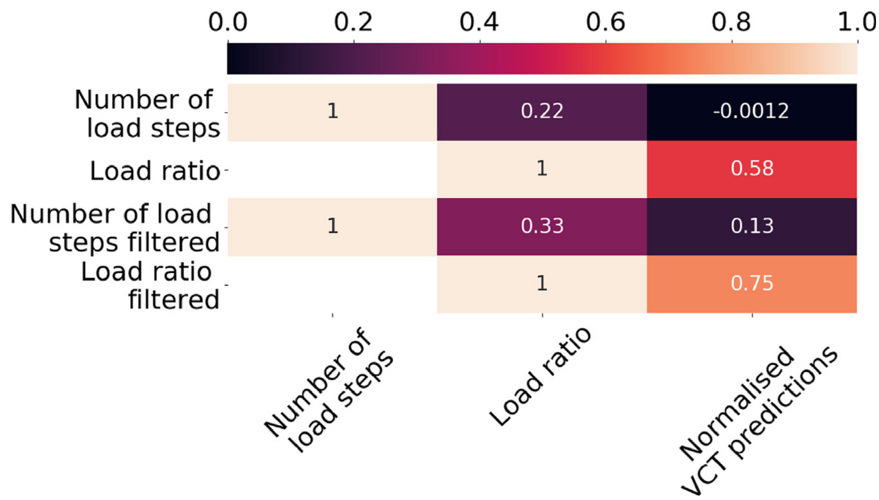

Fig. 4. Kendall's correlation analysis, pristine numerical data.

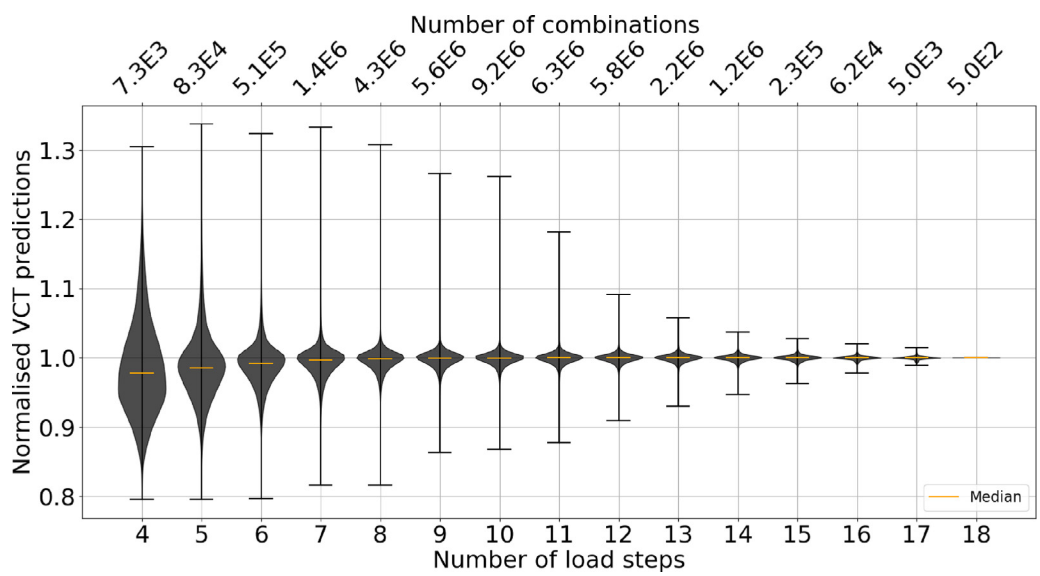

Fig. 5. VCT predictions as a function of the number of load steps with random frequency deviations within ±0.1 Hz.

the weak correlation is artificially introduced by the filtering criteria. On the other hand, the correlation coefficients between the maximum load levels and the VCT buckling load predictions indicates a strong correlation between the two, the higher one for the filtered load steps being also introduced by the filtering criteria. This implies that, in ideal conditions, the VCT buckling load predictions are only influenced by the maximum load ratio of the measurements, while the number of load steps measured has no influence whatsoever over the predictions.

3.3. Sensitivity study with frequency deviations

The previous study revealed that the number of load steps used has little influence over the VCT buckling load predictions and that the maximum load level is the main parameter that influences these predictions. This study however was a representation of the ideal case, as it was based on pure numerical data from nominally identical cylinders, where the obtained load–frequency data followed with high fidelity a quadratic response. In practice, random vibration mode frequency measurement deviations can occur, resulting in a poorer quality of the quadratic fits, like the ones shown in Fig. 1. Therefore, the influence of frequency measurement deviations must also be accounted for when studying the influence of the number of load steps and the maximum load ratio over the VCT buckling load predictions.

3.3.1. Influence of ±0.1 Hz frequency deviations

Fig. 5 shows the violin plots of the numerical VCT predictions for the 50 altered data sets generated with a maximum allowed vibration frequency deviation within ±0.1 Hz, as a function of the number of load steps.

When comparing this figure with its analogue Fig. 2 for the ideal scenario (case with filtered load steps), some clear differences can be found. While in Fig. 2 the VCT predictions varied by small amounts (0.91–1.03), here the variations are considerably larger (0.8–1.35), this variation being larger on the upper limit. However, the amplitude of the variations drops significantly with increasing the number of load steps beyond 10, with a tendency to stabilise to a quasi-linear decrease beyond 12 load steps. Furthermore, the predictions clusters seem to stabilise sooner around the same value. The small amplitude of the clustered VCT predictions when compared to the amplitude of the extremes also implies that the number of the predictions outside these clusters is negligible compared with the number of the ones within. Therefore, the values outside these clusters can also be considered as outliers given by the frequency deviations introduced. For this frequency deviation magnitude, the clustered predictions are well within ±0.1 when more than 4 load steps are used, meaning that using just 5 load steps gives a relative deviation of ±10% with respect to using all the load steps

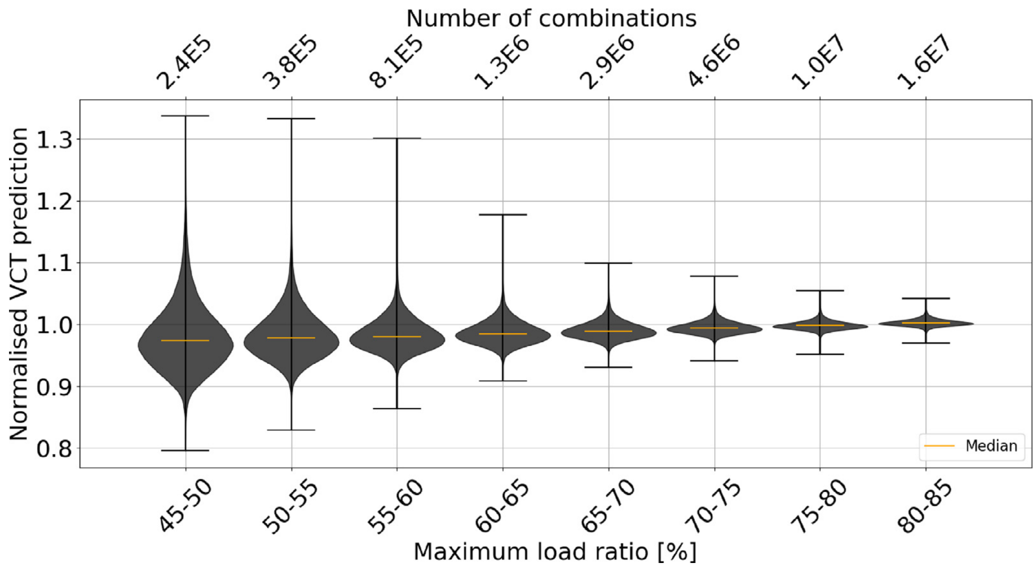

Fig. 6. VCT predictions as a function of the maximum load ratio with random frequency deviations within ±0.1 Hz.

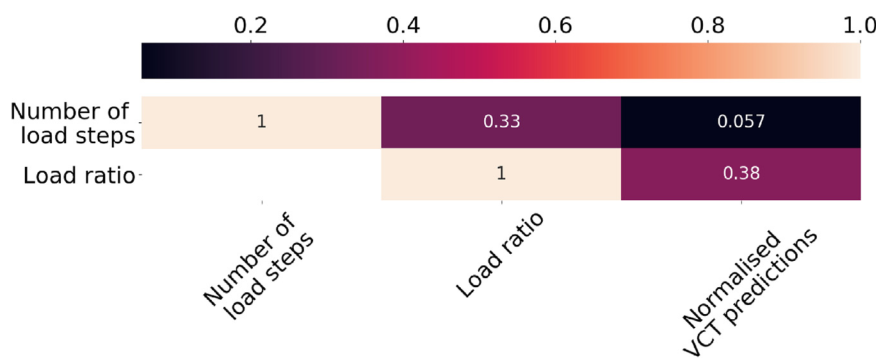

Fig. 7. Kendall's correlation data analysis with random frequency deviations within ±0.1 Hz.

available. The clusters' amplitude decreases rapidly with increasing the number of load steps at the beginning, being in the limits of (0.95–1.03) when more than 6 load steps were used.

Remembering that the influence of the number of load steps is not entirely decoupled from the maximum load level used and that the load criteria automatically impose a maximum load ratio between 50% and 85%, the maximum load ratio used can also influence these results. This aspect can be verified by checking if significant range decreases between consecutive maximum load ratios are present in Fig. 6, where the violin plots are shown as a function of the maximum load ratio used. Inspecting this figure reveals only gradual cluster range decreases between consecutive maximum load ratio intervals, suggesting that in this case indeed when using more than 4 load steps, with a maximum load ratio higher than 55%, the influence of the introduced frequency deviations for the VCT predictions can highly decrease (cluster range within ±0.1). Furthermore, when comparing this figure with its analogue Fig. 3 for the ideal case with load steps criteria, one can observe that now a relation between the maximum load levels used and the VCT predictions is no longer as evident. Inspecting the extreme VCT predictions from Figs. 5 and 6 and comparing them with the extremes predictions from Figs. 2 and 3 for the ideal case shows that the introduction of the frequency deviations also influenced the maximum load ratio needed to obtain these extreme values.

For this magnitude of the frequency deviations, the highest VCT predictions were no longer obtained when using the highest load ratio available, but the lowest. This can have an important impact on the robustness of the VCT predictions in the presence of such deviations, as there is an increased risk that the predictions would be over-conservative, even when having a relatively low maximum load ratio.

The Kendall's correlation coefficient is also used here, Fig. 7 showing the correlations for these data sets. When comparing Fig. 7 with Fig. 4, one can notice that the frequency deviations introduced decreased the correlation between the maximum load level used and the VCT predictions by roughly half, from 0.75 to 0.38. While this correlation coefficient decreased by a significant amount, it still indicates a relatively strong correlation between the maximum load level and the VCT predictions.

As expected, the correlation coefficient between the number of load steps used and the VCT predictions is now showing no correlation whatsoever, despite the influence of this parameter on the VCT prediction range. This change is due to the multiple data sets used, where any artificial correlation between these two parameters for a particular data set is compensated by the other data sets. Also as expected, the correlation between the number of load steps and the maximum load ratio used is still 0.33, as the magnitude of the introduced frequency deviations should have no influence over this correlation.

3.3.2. *Influence of ±0.25 Hz frequency deviations*

Fig. 8 shows the VCT predictions as a function of the number of load steps used for frequency deviations within ±0.25 Hz.

As it can be seen from this figure, now the clusters range of the VCT predictions become relatively constant and within ±0.1 when using more than 6 load steps. Also, the number of load steps range that gives the highest VCT predictions increased from 4–10 to 4–12, while the lowest predictions were still obtained using a low number of load steps.

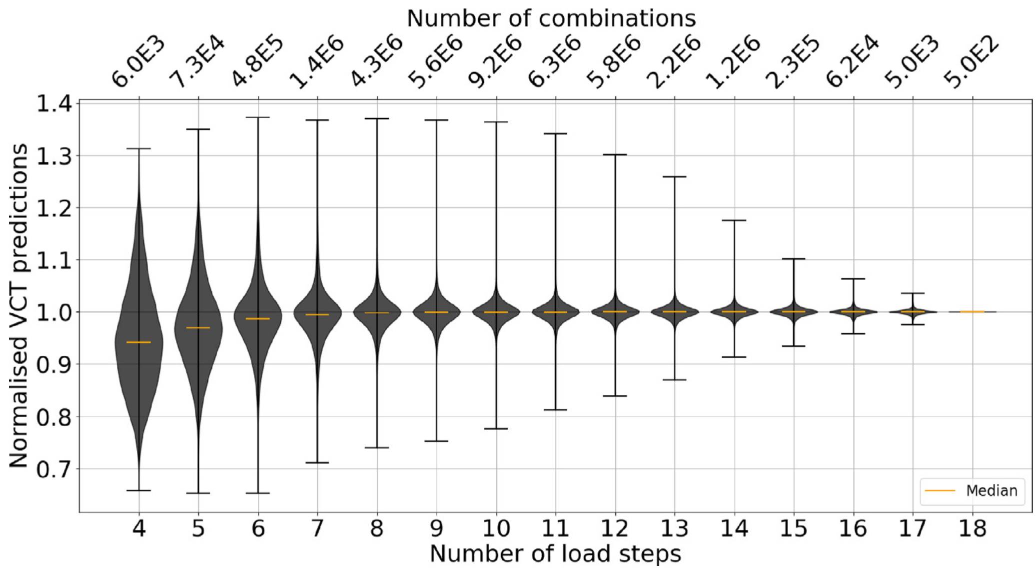

Fig. 8. VCT predictions as a function of the number of load steps with random frequency deviations within ±0.25 Hz.

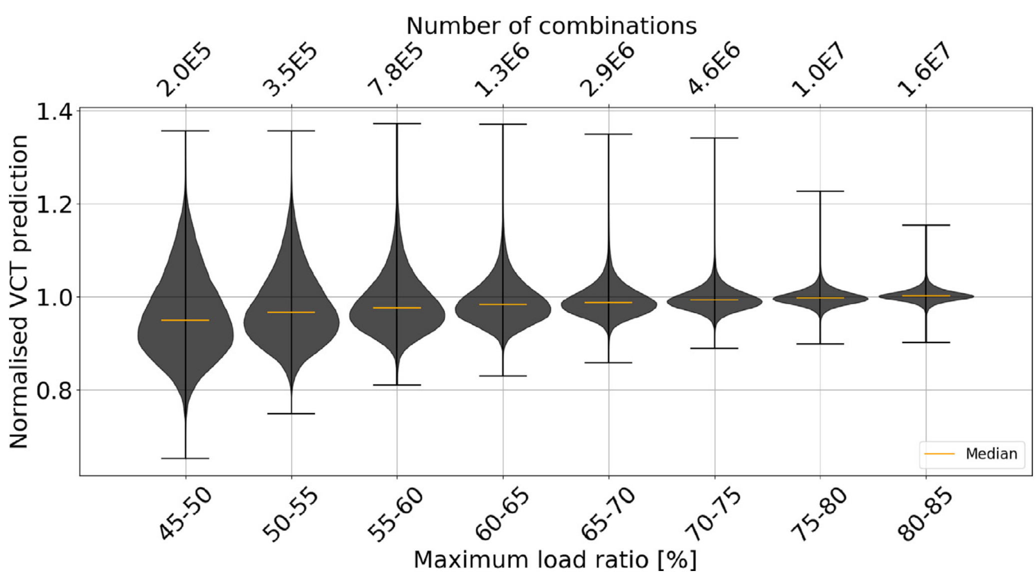

Fig. 9. VCT predictions as a function of the maximum load ratio with random frequency deviations within ±0.25 Hz.

Regarding the maximum load ratios of the predictions at the extremes, Fig. 9 shows that the highest VCT predictions were obtained for a larger maximum load ratios interval, between 50% and 75%, while previously these were found between 50% and 55%. Furthermore, the cluster ranges also increased by a small amount, now the load ratio after which cluster range becomes within ±0.1 is from 65% onwards. On the other hand, the lowest predictions were still obtained using the lowest load ratio available.

Fig. 10 shows the correlation coefficients for the VCT predictions with frequency measurement deviations within ±0.25 Hz.

When comparing this figure with its analogue Fig. 4 for the ideal case with filtered load steps and Fig. 7 for a deviation magnitude within ±0.1 Hz, it can be seen that the increased deviation magnitude seemed to significantly alter the correlation between the load level and the VCT predictions. Now the correlation coefficient halved again, from 0.38 to 0.19 and although this value still indicates that a correlation exists, this correlation is now weak. On the other hand, the correlation between the number of load steps and the VCT predictions remained the same.

3.3.3. *Influence of ±0.5 Hz frequency deviations*

Fig. 11 shows the VCT predictions as a function of the number of load steps when frequency deviations within ±0.5 Hz are introduced. Here it can be seen that the trends observed before continue. For this deviation magnitude, the necessary number of load steps to reduce the VCT predictions cluster range increased to more than 8. The upper limit of the number of load steps that can give the highest predictions also increased to 13, while the number of load steps for the lowest predictions is from 3 to 5 load steps.

Fig. 12 shows the VCT predictions as a function of the load ratio used for frequency deviations within ±0.5 Hz. In this figure, it can be observed that the load ratio range over which the highest predictions occur changed. The highest predictions can now be found at any load ratio, while the lowest predictions were still found at the minimum load ratio. Moreover, the clusters now become stable and roughly within ±0.1 after a 75% load ratio, larger by 10% than for frequency deviations within ±0.25 Hz.

The frequency deviations within ±0.5 Hz introduced deterred even more the correlation between the VCT predictions and the maximum

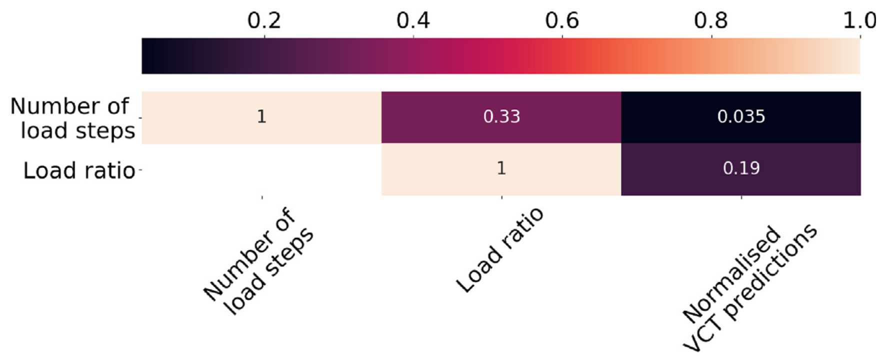

Fig. 10. Kendall's correlation data analysis with random frequency deviations within ±0.25 Hz.

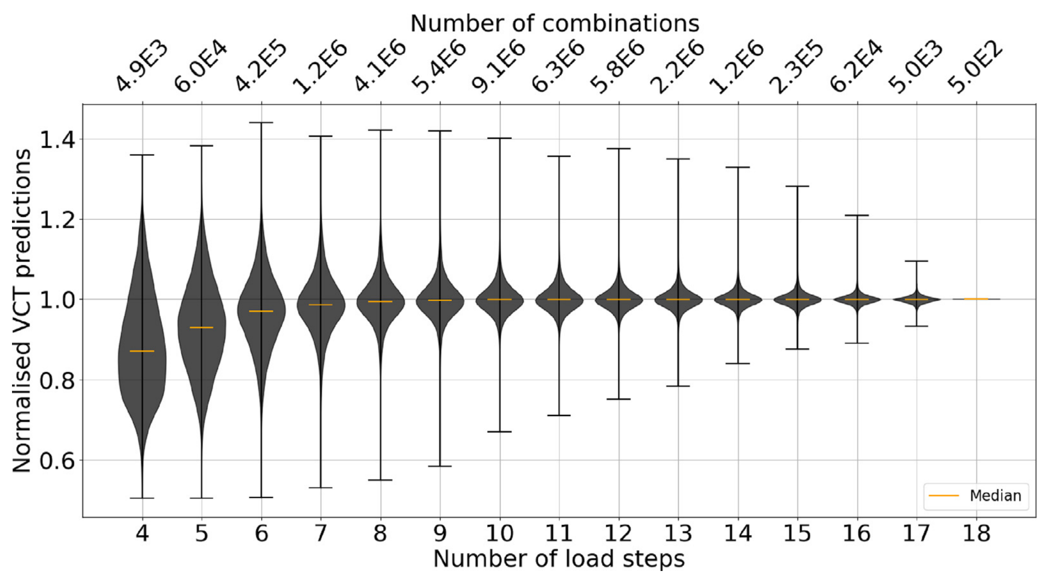

Fig. 11. VCT predictions as a function of the number of load steps with random frequency deviations within ±0.5 Hz.

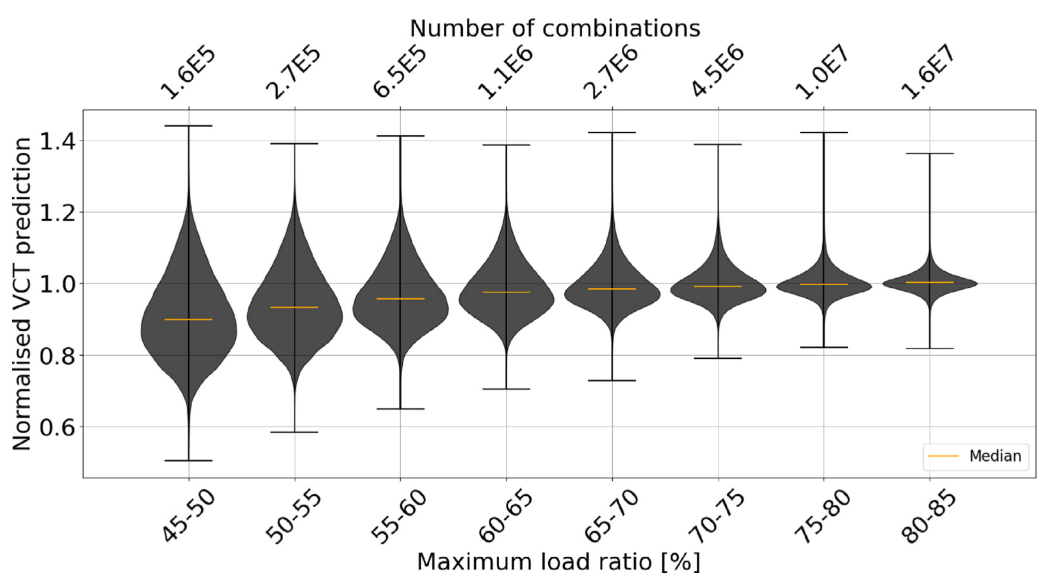

Fig. 12. VCT predictions as a function of the maximum load ratio with random frequency deviations within ±0.5 Hz.

load level. This can be seen from Fig. 13, where now the Kendall correlation coefficient is 0.12, describing a very weak correlation.

The sensitivity study based on the FE results suggested that there is a strong positive correlation between the VCT predictions and the maximum load ratio used and that the introduced frequency deviations heavily altered this correlation. Furthermore, the maximum load ratio needed to reduce the clusters amplitude within ±0.1 also increased with increasing the magnitude of the introduced frequency deviation. On

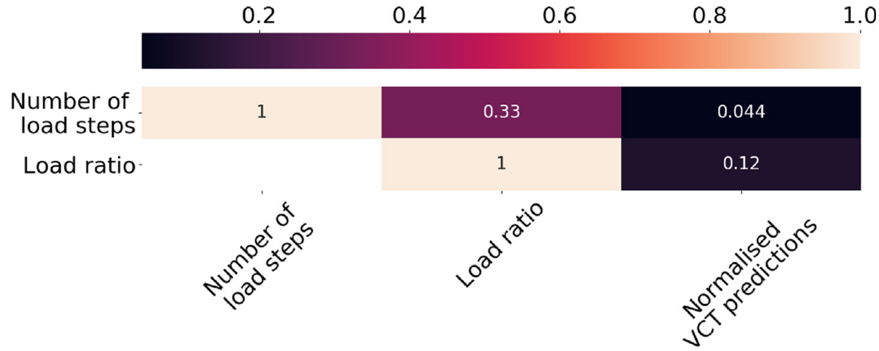

Fig. 13. Kendall's correlation data analysis with random frequency deviations within ±0.5 Hz.

Table 3
Cylinders used for the experimentally based sensitivity study.

Name	Mat	h [mm]	D [mm]	t [mm]	r/t	AR
Ghahfarokhi grid* [29]	GFRP	300	160	1.2	66	1.9
Ghahfarokhi grid 2* [30]	GFRP	300	160	1.5	32	1.9
Labans classic tow [28]	CFRP	790	600	1.45	207	1.3
Labans variable tow [28]	CFRP	835	600	1.45	207	1.4
R07 [24]	CFRP	500	500	0.63	399	1.0
R08 [24]	CFRP	500	500	0.63	399	1.0
R09 [24]	CFRP	500	500	0.63	399	1.0
R15 [26]	CFRP	500	500	0.52	478	1.0
D100H200L1-HS (1, 2) [31,32]	CFRP	200	100	0.29	170	2.0
D100H200L1-PP (3-9) [31,32]	CFRP	200	100	0.29	170	2.0
D100H200L2 (1-3, 3a, 5) [32]	CFRP	200	100	0.27	183	2.0
D100H400L1-HS (1-3) [31,32]	CFRP	400	100	0.3	168	4.0
D100H400L1N-PP (4-6) [31,32]	CFRP	400	100	0.3	168	4.0
D100H400L2 (2) [32]	CFRP	400	100	0.36	141	4.0
D300H150L1 (1, 3) [32]	CFRP	150	300	0.36	418	0.5
D300H150L1-HS (2) [31,32]	CFRP	150	300	0.36	418	0.5
D300H150L2 (1) [32]	CFRP	150	300	0.36	418	0.5
D300H150L2N (3) [32]	CFRP	150	300	0.36	418	0.5
D300H150L1N-PP (5) [31,32]	CFRP	150	300	0.36	418	0.5
D300H300L1-PP (3) [31,32]	CFRP	300	300	0.34	446	1.0
D300H300L1N-PP (4, 5) [31,32]	CFRP	300	300	0.34	446	1.0
SST1 [26]	Al	500	500	0.5	500	1.0
SST2 [26]	Al	800	800	0.5	800	1.0
Z37 [26]	CFRP	800	500	0.79	318	1.6
Z38*, ** [23]	Al	1000	801	2.18	183	1.2
ZD27 [27]	CFRP	560	502	0.58	432	1.1
ZD28 [27]	CFRP	560	502	0.48	523	1.1
ZD29 [27]	CFRP	560	502	0.52	482	1.1

the other hand, the influence of the number of load steps used on the VCT predictions was relatively weak, with increasing the number of load steps mainly reducing the magnitude of the errors given by the introduced frequency deviations.

4. Experimental results

While some clear trends on the influence of the number of load steps and the maximum load ratio were observed on the sensitivity study based on FE results, these trends were based exclusively on a family of nominally identical cylinders. Therefore, for confirming these trends, a sensitivity study based on experimental results was also performed.

For the experimental results, a thorough literature review was performed, gathering a fairly large number of published measurements. These measurements are for cylinders out of different materials (Steel, Al, GFRP, CFRP), diameters D (160 mm–801 mm), heights h (150 mm–1000 mm), shell thicknesses t (0.273 mm–2.5 mm), r/t (32–800), aspect ratios AR (0.5–4), boundary conditions, loading, or with/without stiffening. Table 3 shows the geometrical data of the cylinders used for this sensitivity study, where PP/HS relates to the load introduction (Parallel Plates/SemiSpherical joint), * represents stiffened cylinders and ** represents cylinders tested with internal pressure.

These cylinders were used together in this study, regardless of their material, structural and geometrical differences, in order to assess the sensitivity of the method including not only a large variety of cylinders, but also a large number, namely 48 VCT data sets, from 28 nominally different cylinders. The difference from 28 nominally different cylinders to 48 different VCT data sets comes from the fact that some of the cylinders were tested with internal pressure, or with different load introduction methods.

While for the numerical study the number of the load steps and the load ratios of the measurements can be accurately controlled, due to the unpredictability of the buckling event, same is not the case for the experimental data. The raw experimental data of the cylinders shown on the above table contained a different number of measurements, at different load ratios and for a different number of vibration modes. This raised several issues in trying to use the data in a similar way as for the numerical study. Given the fact that for some cylinders there were multiple vibration modes monitored and/or a larger number of measurements when compared to others, using these measurements in their raw form would introduce a huge bias towards these cylinders. For example, in the work of Labans et al. [28] there were 4 vibration modes monitored over 16–17 load steps, while in the work of Arbelo et al. for the R09 cylinder [24] the published data was only for the first vibration mode, over only 7 load steps. This meant that, when using an identical approach as for the numerical study, the results using the complete data from [28] would represent more than 80% of our entire data. In order to increase the influence of the other cylinders, only the first vibration mode was used for the VCT predictions and the number of load steps was reduced to a maximum of 14. For the cylinders with more than 14 valid measurements published, the number of load steps reduction was performed such that the minimum and maximum load ratios were not influenced and by avoiding removing consecutive measurements. After this reduction, the highest contribution of any cylinder to the total amount of data was around ∼10%, for 7 data sets having the maximum number of load steps of 14. This meant that 7/48 data sets (∼15%) gave roughly 70% of the results and the rest of 41/48 data sets (∼85%) gave roughly 30% of the results. While the contribution of the cylinders to the total amount of VCT buckling load predictions greatly differs from one cylinder to another, the data sets with a higher number of load steps were kept, such that the influence of this parameter can be properly assessed using the experimental VCT data as well.

4.1. Sensitivity study

Fig. 14 shows the violin plots of the predictions as a function of the number of load steps used for the experimental VCT predictions without any frequency deviations introduced.

When compared to the numerical counterparts, one can notice that more features are shared with Figs. 5, 8 and 11 for frequency deviations within ±0.1 Hz, ±0.25 Hz and ±0.5 Hz, rather than with Fig. 2 for the pristine case and without load criteria. Since for the experimental data the load criteria were not used, the most extreme predictions

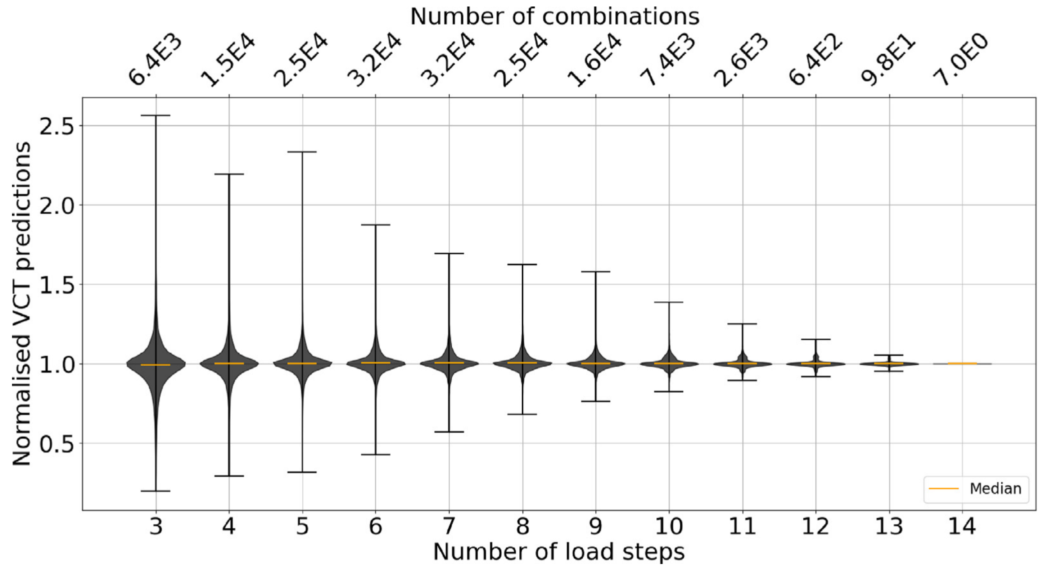

Fig. 14. VCT predictions as a function of the number of load steps, pristine experimental data.

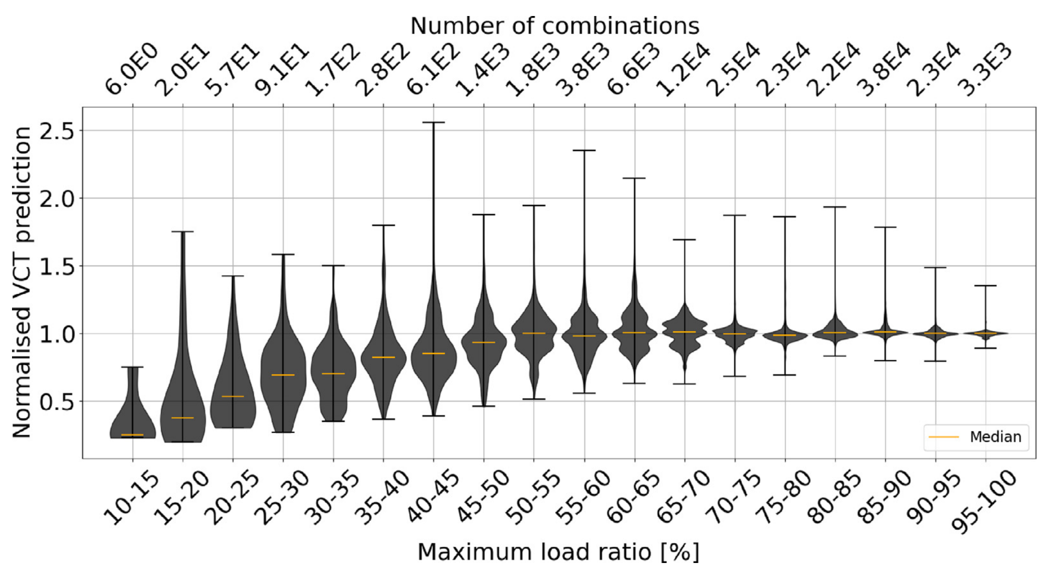

Fig. 15. VCT predictions as a function of the maximum load ratio, pristine experimental data.

were found for the lowest number of load steps, like in Fig. 2 for the numerical predictions without load criteria applied. On the other hand, the amplitudes given by both the extreme predictions, as well as the ones of the clusters resemble more the numerical results with frequency deviations included, as the experimental data would naturally include a certain degree of such deviations. However, the amplitude in this case is roughly 2.5 larger than for the numerical case where ±0.5 Hz frequency deviations were introduced. A closer investigation revealed that the extremely high values were exclusively given by the data set of the SST-2 cylinder [26], these types of results being only possible when a set of 2 conditions are met. These conditions are: **(i)** a very low VCT buckling knock-down factor, here 0.29; and **(ii)** load steps combinations that give VCT predictions close to the linear buckling load P_{cr}. In other words, these high normalised values are found when an intermediate VCT prediction that is relatively close to the linear buckling load is divided by such a low knock-down factor given by the nominal VCT prediction (when using all the measurements). Using this data one can find the knock-down factor of the intermediate VCT prediction that gave a normalised prediction of ~2.5, by simply multiplying the two, giving a value of 0.725. Regardless, the data set of this cylinder was kept in this study, as the VCT buckling load prediction error was within 5% of the experiment.

Fig. 15 shows the same VCT predictions as the ones in Fig. 14, but rearranged as a function of the load ratio.

Here the predictions were grouped in load ratio intervals of 5%, same as for the previous numerically based sensitivity study, as the experimental load ratios varied greatly between different cylinders. Similar to the case where the predictions were shown as a function of the number of load steps used, this figure also resembles more the equivalent figures for numerical cases where frequency deviations were included. This is due to the fact that also here the clustered predictions tend to stabilise after a certain load ratio. The amplitude of these clusters is similar to the last numerical case for the same load ratios (higher than 50%), suggesting that the magnitude of the frequency deviations introduced in the numerical study was appropriate. Moreover, also the load ratio after which the cluster range fits within ±0.1 is for load ratios higher than 70%, which is very similar to the case based on FE results with frequency deviations within ±0.5 Hz introduced.

One of the differences between the analysis based on experimental results and the one based on numerical results is that, in the former,

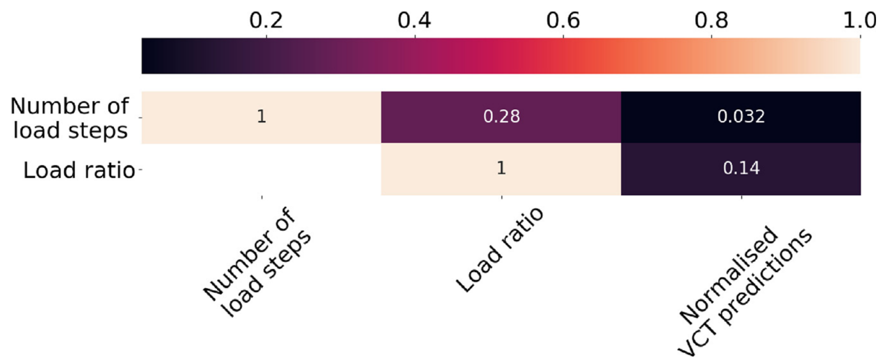

Fig. 16. Kendall's correlation analysis, pristine experimental data.

the clusters have different shapes, especially for lower load ratios, as they incorporate multiple nominally different cylinders. This is also the reason why the number of combinations is no longer constantly increasing with the load ratio used, given that the experimental data of the used cylinders has a different number of load steps and different maximum load ratios.

For the experimental data sets, since for different cylinders the normalised VCT predictions tend towards 1 with different gradients, simply merging all data sets together and performing the correlation on the combined data set would give erroneous results. Instead, for the experimental data the correlation was performed individually for each cylinder and then these coefficients were averaged. Fig. 16 shows a heatmap of the averaged Kendall correlation coefficients for the pristine experimental data.

Here it can be seen that also for the experimental data there is a weak correlation between the load ratio and the number of load steps and no correlation between the predictions and the number of load steps. However, there is a significant difference between using the numerical data and the experimental one to perform the correlation between the load ratio and the VCT predictions. While for the numerical data there is a strong correlation between the load ratio and the predictions, for the numerical data this correlation seems to be weak, this coefficient being closer to the one for the numerical case where frequency deviations within ±0.5 Hz were introduced.

4.2. Sensitivity study with frequency deviations

The previous study showed again that the number of load steps used has little influence over the VCT buckling load predictions, while the influence of the load ratio appeared to be weak. While some frequency deviations are likely present in the measured data, also for the experimental data the same frequency deviations magnitudes within ±0.1 Hz, ±0.25 Hz and ±0.5 Hz were introduced to study the sensitivity of the VCT method to the number of load steps and load ratio when altering the measured frequencies. Given the negligible differences found when introducing the frequency deviations, here only the results for frequency deviations within ±0.5 Hz are shown.

4.2.1. Influence of ±0.5 Hz frequency deviations

Fig. 17 shows the violin plots of the VCT predictions for the data sets generated with a maximum allowed vibration frequency deviation within ±0.5 Hz, as a function of the number of load steps. When comparing this figure with its analogue Fig. 14 for the experimental results without frequency deviation introduced, one can notice that the biggest difference is the larger amplitude of the predictions, particularly for a lower number of load steps. Also, while the amplitude of the extreme predictions was significantly increased, the amplitude of the clusters slightly decreased, despite the frequency deviations introduced. While this behaviour could seem counter-intuitive, the explanation comes from the higher number of data sets used. Since most of the VCT predictions of each cylinder are around the median, using 50 altered sets for each cylinder meant that the number of the clustered predictions increased faster than the ones outside, which is the reason why the amplitude of the clusters decreased.

Fig. 18 shows the experimental VCT predictions as a function of the load ratio used for frequency deviations within ±0.5 Hz. Similarly as for the previous plot, here the ranges of the clusters also decreased when compared to the results using pristine experimental data, owing to the same larger number of data sets used. The medians of the distributions seem to stabilise also around 1 and the significant amplitude decrease still occurs for load ratios higher than 70%. Perhaps one of the most significant changes with respect to the pristine results (besides the cluster amplitude decrease) is that now the extremely high predictions appear to be randomly found at multiple load ratios. Regardless, these can be considered as minor changes, suggesting that the introduced frequency deviations in the experimental data sets do not influence greatly the VCT predictions.

The Kendall's correlation coefficient was also used here, Fig. 19 showing the averaged correlation coefficients for these data sets. When comparing this figure with Fig. 16, one can notice that the frequency deviations introduced barely altered any of the coefficients, giving support to the negligible influence of the introduced frequency deviations over the VCT predictions using the experimental data.

5. Discussion

The sensitivity study based on FE results suggested that there is no monotonic relation between the number of load steps and the VCT prediction, but that increasing the number of load steps could reduce the influence of present frequency deviations. On the other hand, a strong monotonic relation was found between the maximum load ratio and the VCT predictions, the strength of this monotonic relation decreasing with increasing the magnitude of the frequency deviation introduced. Furthermore, it suggested that the extreme predictions are likely found when using a relatively low number of load steps, all at extreme load ratios, with the low load ratios giving the lowest VCT predictions, while the highest load ratios give the highest VCT predictions.

The sensitivity study based on experimental results confirmed most of the trends observed from the numerical study, with one major difference. This difference was observed in the correlation between the maximum load ratio and the VCT prediction, which slightly increased, instead of decreasing, with increasing the magnitude of the frequency deviations introduced in the experimental data. A deeper investigation on these averaged correlation coefficients showed that this difference came from several cylinders for which the VCT predictions converged 'from below'. In other words, in several data sets the VCT prediction highly decreased with increasing the load ratio. This meant that for these cylinders the correlation coefficients were negative, which when averaged highly decreased the overall correlation coefficient. Moreover, these data sets were also responsible for the small increase of

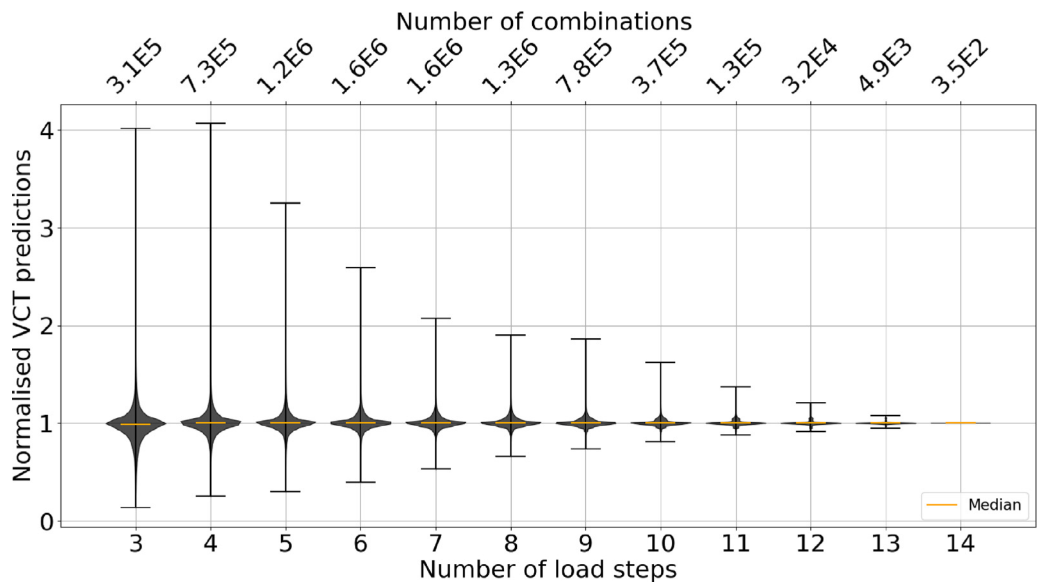

Fig. 17. VCT predictions as a function of the number of load steps with random frequency deviations within ±0.5 Hz.

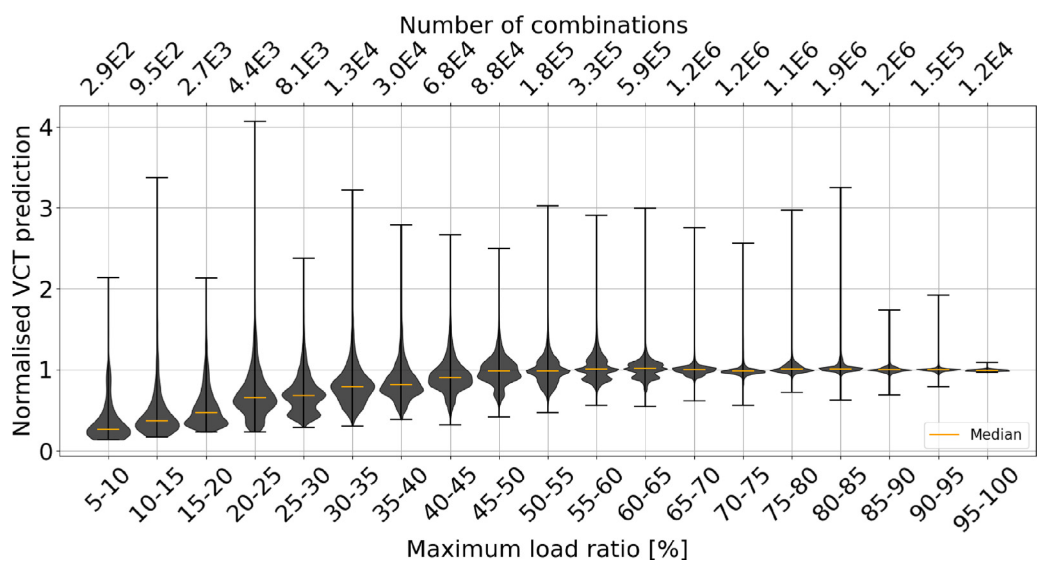

Fig. 18. VCT predictions as a function of the maximum load ratio with random frequency deviations within ±0.5 Hz.

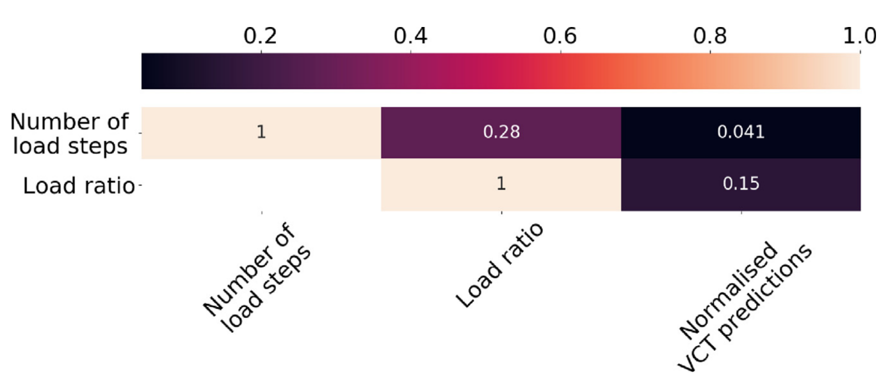

Fig. 19. Kendall's correlation data analysis with random frequency deviations within ±0.5 Hz.

the correlation coefficient between the VCT prediction and the load ratio when increasing the magnitude of the introduced frequency deviation. A closer inspection over the results of each data set individually revealed that the increase of the negative correlation coefficients was higher than the decrease of the positive correlation coefficients. This higher magnitude in the increase of the negative correlation coefficient was sufficient to overcome the lower magnitude decrease of the positive correlation coefficient, which translated in the small increase in the overall correlation coefficient with increasing the magnitude of the frequency deviation introduced. Furthermore, given the higher number of available VCT predictions for higher load ratios, the coefficient relating the maximum load ratio with the VCT prediction also contains a bias towards the results from higher load ratios. This is also one of the reasons why some of the coefficients were negative, despite a clear positive correlation between the two parameters, particularly for load ratios below 50%.

The correlation coefficients for all the experimental data varied from −0.64 to 0.77 depending on the cylinder and generally suffered only minor changes when frequency deviations were introduced. This difference with respect to the numerical data could be explained by the difference between the relative magnitude of the frequency deviation introduced and the magnitude of the frequency drop with increasing the load in the experiments. For example, for the study based on FE results the frequency change between two consecutive load steps was around 3 Hz, meaning that the ±0.5 Hz deviation introduced could change this gap by ±1 Hz (±33%). While similar frequency gaps were also seen in the experimental results, for most of these data sets this gap was larger, meaning that also the magnitude of the frequency deviations introduced disturbed less these gaps. This difference in the frequency gap between the numerical and the experimental sets can come from two sources: **(i)** the magnitude of the frequency drop between the first and the last load step used; and/or **(ii)** the spacing between the consecutive load steps. Exemplifying, for the same first and last load ratios of 10% and 80% respectively, for the methodology used here having 10 equally spaced load steps in between would yield, provided that the VCT method converges 'from above', a higher correlation between the load ratio and the VCT prediction than compared to the case where 20 equally spaced load steps would be used. This is due to the increased risk that the measurements of two consecutive load steps could give relatively close natural frequencies, which would further give two points close to each-other, like the ones from Fig. 1, thus hampering a quadratic curve fit.

6. Conclusions

In this paper, a study on the influence of the number of load steps and of the maximum load level used for predicting buckling loads of cylindrical shells using VCT is presented. The study contained both a sensitivity study based on numerical results of a family of nominally identical, validated through experiment FE models, as well as one based on experimental results gathered from the literature. Using this numerical and experimental data, multiple combinations of load steps were generated to assess the sensitivity of the VCT for buckling load prediction to the number of load steps and the maximum load ratio used. The study revealed that, when frequency deviations were not artificially introduced in the numerical data, there was a strong positive monotonic relation between the maximum load ratio and the VCT predictions. Reliability-based VCT predictions that are more representative of the reality were carried out by including random frequency measurement deviations within ±0.1 Hz, ±0.25 Hz and ±0.5 Hz. It was found that: **(i)** the strength of the monotonic relation between the load ratio and the VCT predictions decreased with increasing the magnitude of the deviation; and **(ii)** increasing the number of load steps mostly decreased the influence of the introduced deviations. Furthermore, the distributions of the VCT predictions tended to become narrower with increasing the load ratio, regardless of the number of load steps used. This occurs since the usage of measurements at higher load ratios tends to prevent over-conservative predictions. Also, the variation of the VCT predictions tends to decrease with increasing the maximum load ratio, regardless of the number of load steps used. This can be seen in the main clusters of the VCT predictions from each violin plot shown in this study. Moreover, as the VCT predictions tend to cluster, with the bulk of the predictions around the same value, the predictions outside these clusters can be considered as outliers given by the frequency deviations introduced. The introduced deviations also had an influence over the importance of the number of load steps used for the predictions. While the correlation between the number of load steps and the VCT prediction was non-existent, it was found that, depending on the magnitude of the introduced deviation, there is a number of load steps after which the influence of the deviations over the predictions range significantly reduces. This can be important in designing an experimental test since, if the maximum magnitude of the expected frequency measurement deviations is known, performing such studies will give a minimum number of load steps for which the influence of these deviations could be greatly reduced.

The numerical sensitivity study proved to be relevant in showcasing multiple trends of the VCT prediction as a function of the number of load steps and load ratio used, as most of the observations made for this study were relevant for the sensitivity study based on experimental data. However, there was an important difference in the evolution of the VCT predictions as a function of the load ratio between the sensitivity study based on the numerical data and the one based on the experimental data. While there was a strong monotonic relation between the VCT prediction and the load ratio used for the numerical based data, for the experimentally based data the strength of this relation appeared to be weak. Moreover, also the influence of the artificially introduced deviation on the strength of this monotonic relation was found to be opposite between the two types of data. While increasing the magnitude of these deviations highly deterred the good correlation for the numerically based data, for the experimentally based data the weak correlation was slightly improved. This difference came from several cylinders for which the VCT method converged 'from below', meaning that the VCT prediction dropped for increasing the load ratio. Thus, the correlation coefficients for these sets were negative and severely decreased the overall correlation coefficient. The source of the different influence of the magnitude of the introduced deviation over the numerical and experimental based data was also found to be given by these data sets for which the VCT predictions decreased with increasing the load ratio. For these sets the correlation coefficient increased with increasing the magnitude of the frequency deviation and since the increase of these coefficients was significantly larger than the decrease of the others, the averaged coefficient slightly increased as well.

A closer inspection over the evolution of the correlation coefficients for each individual cylinder data set also revealed that the VCT predictions based on experimental data appears to be less sensitive to frequency deviations than the VCT predictions based on the FE results. This behaviour is assumed to be given by the different magnitude in which the introduced deviations influence the FE and the experimental results, owing to the different load ratio of the consecutive load steps and the different total frequency drop between the first and the last load step.

Given the significant diversity of cylinders, as well as their loading and testing boundary conditions, the trends identified in the present study are likely to be valid for other imperfection-sensitive structures and cylindrical shells in particular. Furthermore, when used for a single test case, or a family of nominally identical structures, the methodology used here for the sensitivity study could also be used to define a robust number of load steps and maximum load ratio to be tested, such that the influence of frequency deviations of a certain magnitude is alleviated.

CRediT authorship contribution statement

Theodor D. Baciu: Visualization, Validation, Software, Methodology, Investigation, Formal analysis, Data curation, Conceptualization, Writing – original draft, Writing – review & editing. **Richard Degenhardt:** Supervision, Resources, Project administration, Funding acquisition, Data curation, Investigation, Methodology, Writing – review & editing. **Felipe Franzoni:** Supervision, Software, Conceptualization, Data curation, Methodology, Writing – review & editing. **Adrian**

Gliszczynski: Supervision, Investigation, Methodology, Writing – review & editing. **Mariano A. Arbelo:** Investigation, Methodology, Writing – review & editing. **Saullo G.P. Castro:** Investigation, Methodology, Writing – review & editing. **Kaspars Kalnins:** Investigation, Methodology, Writing – review & editing.

Declaration of competing interest

The authors declare that they have no known competing financial interests or personal relationships that could have appeared to influence the work reported in this paper.

Data availability

Data will be made available on request.

Acknowledgements

The research leading to these results has received funding from the European Community's Eighth Framework Programme (FP8/H2020), under Priority ERDF (European Regional Development Fund), Grant Agreement Number ZW 6–85042584 and from the Latvian Council of Science, Latvia, grant number LZP-2018/2-363. All support is gratefully acknowledged. The information in this paper reflects only the author's views and the European Community is not liable for any use that may be made of the information contained therein.

References

[1] H. Abramovich, Stability and Vibrations of Thin-Walled Composite Structures, Woodhead Publishing, 2017.
[2] J. Horák, G.J. Lord, M.A. Peletier, Cylinder buckling: The mountain pass as an organizing center, SIAM J. Appl. Math. 55 (2006) 1793–1824, http://dx.doi.org/10.1137/050635778.
[3] J.W. Hutchinson, J.M.T. Thompson, Imperfections and energy barriers in shell buckling, Int. J. Solids Struct. 148 (2018) 157–168, http://dx.doi.org/10.1016/j.ijsolstr.2018.01.030.
[4] J.M.T. Thompson, J.W. Hutchinson, J. Sieber, Probing shells against buckling: A nondestructive technique for laboratory testing, Int. J. Bifurcation Chaos 27 (14) (2017) http://dx.doi.org/10.1142/S0218127417300488.
[5] R.V. Southwell, On the analysis of experimental observations in problems of elastic stability, Proc. R. Soc. London. Ser. A 165 (828) (1932) 601–616, http://dx.doi.org/10.1098/rspa.1932.0055.
[6] W.H. Horton, E.M. Nassar, M.K. Singhal, Determination of the critical loads of shells by nondestructive methods, Exp. Mech. 17 (4) (1977) 154–160, http://dx.doi.org/10.1007/BF0232421.
[7] A. Somerfeld, Eine einfache Vorrichtung zur Veranschaulichung des Knickungsvorganges, Z. Ver. Dtsch Ing. 49 (1905) 1320–1323.
[8] Melan, H, Kritische drehzahlen von wellen mit langsbelastung, Zeitschrijt Osterr Lngenieur- Arch. Vereines 69 (1917) 610–612, 619–621.
[9] H. Lurie, Lateral vibrations as related to structural stability, ASME J. Appl. Mech. 19 (1952) 195–204, http://dx.doi.org/10.1115/1.4010446.
[10] E.E. Johnson, B.F. Goldhammer, The determination of the critical load of a column or stiffened panel by the vibration method, Proc. Soc. Exp. Stress Anal. 11 (1) (1953) 221–232.
[11] M. Chaves-Vargas, A. Dafnis, H.-G. Reimerdes, K.-U. Schröder, Modal parameter identification of a compression-loaded CFRP stiffened plate and correlation with its buckling behaviour, Prog. Aerosp. Sci. 78 (2015) 39–49, http://dx.doi.org/10.1016/j.paerosci.2015.05.009.
[12] R. Radhakrishnan, Prediction of buckling strengths of cylindrical shells from their natural frequencies, Earthquake Eng. struct. Dyn. 2 (1973) 107–115, http://dx.doi.org/10.1002/eqe.4290020202.
[13] Y. Segal, Prediction of Buckling Load and Loading Conditions of Stiffened Shells (MSc Thesis), Faculty of Aeronautical Engineering, Technion – Israel Institute of Technology, 1980.
[14] H. Abramovich, The vibration correlation technique – A reliable nondestructive method to predict buckling loads of thin walled structures, Thin-Walled Struct. 159 (2021) 107308, http://dx.doi.org/10.1016/j.tws.2020.107308.
[15] D. Burgreen, End-fixity effect on vibration and instability, Trans. Amer. Soc. Civil Eng. 126 (1) (1961) http://dx.doi.org/10.1061/TACEAT.0008045.
[16] A. Chailleux, Y. Hans, G. Verchery, Experimental study of the buckling of laminated composite columns and plates, Int. J. Mech. Sci. 17 (8) (1975) 489–498, http://dx.doi.org/10.1016/0020-7403(75)90013-2.
[17] M.A. Souza, W.C. Fok, A.C. Walker, Review of experimental techniques for thin-walled structures liable to buckling: Neutral and unstable buckling, Exp. Tech. 7 (9) (1983) 21–25, http://dx.doi.org/10.1111/j.1747-1567.1983.tb01811.x.
[18] H. Abramovich, D. Govich, A. Grunwald, Buckling prediction of panels using the vibration correlation technique, Prog. Aerosp. Sci. 78 (2015) 62–73, http://dx.doi.org/10.1016/j.paerosci.2015.05.010.
[19] M.A. Arbelo, S.F.M. de Almeida, M.V. Donadon, S.R. Rett, R. Degenhardt, S.G.P. Castro, K. Kalnins, O. Ozoliņš, Vibration correlation technique for the estimation of real boundary conditions and buckling load of unstiffened plates and cylindrical shells, Thin-Walled Struct. 79 (2014) 119–128, http://dx.doi.org/10.1016/j.tws.2014.02.006.
[20] F. Franzoni, R. Degenhardt, J. Albus, M.A. Arbelo, Vibration correlation technique for predicting the buckling load of imperfection-sensitive isotropic cylindrical shells: An analytical and numerical verification, Thin-Walled Struct. 140 (2019) 236–247, http://dx.doi.org/10.1016/j.tws.2019.03.041.
[21] E. Skukis, O. Ozolins, J. Andersons, K. Kalnins, M.A. Arbelo, Applicability of the vibration correlation technique for estimation of the buckling load in axial compression of cylindrical isotropic shells with and without circular cutouts, Shock Vib. (2017) http://dx.doi.org/10.1155/2017/2983747.
[22] M.A. Arbelo, A. Herrmann, S.G.P. Castro, R. Khakimova, R. Zimmermann, R. Degenhardt, Investigation of buckling behavior of composite shell structures with cutouts, Appl. Compos. Mater. 22 (2015) 623–636, http://dx.doi.org/10.1007/s10443-014-9428-x.
[23] F. Franzoni, F. Odermann, D. Wilckens, E. Skuķis, K. Kalniņš, M.A. Arbelo, R. Degenhardt, Assessing the axial buckling load of a pressurized orthotropic cylindrical shell through vibration correlation technique, Thin-Walled Struct. 137 (2019) 353–366, http://dx.doi.org/10.1016/j.tws.2019.01.009.
[24] M.A. Arbelo, K. Kalnins, O. Ozolins, E. Skukis, S.G.P. Castro, R. Degenhardt, Experimental and numerical estimation of buckling load on unstiffened cylindrical shells using a vibration correlation technique, Thin-Walled Struct. 94 (2015) 273–279, http://dx.doi.org/10.1016/j.tws.2015.04.024.
[25] E. Skukis, K. Kalnins, O. Ozolins, Application of vibration correlation technique for open hole cylinders, in: Kharkov: Proceedings of the 5th International Conference on Nonlinear Dynamics, Vol. 5, 2016, pp. 377–383, http://repository.kpi.kharkov.ua/handle/KhPI-Press/24830.
[26] K. Kalnins, M.A. Arbelo, O. Ozolins, E. Skukis, Experimental nondestructive test for estimation of buckling load on unstiffened cylindrical shells using vibration correlation technique, Shock Vib. (2015) http://dx.doi.org/10.1155/2015/729684.
[27] F. Franzoni, F. Odermann, E. Lanbans, C. Bisagni, M.A. Arbelo, R. Degenhardt, Experimental validation of the vibration correlation technique robustness to predict buckling of unstiffened composite cylindrical shells, Compos. Struct. 224 (2019) 111107, http://dx.doi.org/10.1016/j.compstruct.2019.111107.
[28] E. Labans, H. Abramovich, C. Bisagni, An experimental vibration-buckling investigation on classical and variable angle tow composite shells under axial compression, J. Sound Vib. 449 (2019) 315–329, http://dx.doi.org/10.1016/j.jsv.2019.02.034.
[29] D. Shahgholian-Ghahfarokhi, G. Rahimi, Buckling load prediction of grid-stiffened composite cylindrical shells using the vibration correlation technique, Compos. Sci. Technol. 167 (2018) 470–481, http://dx.doi.org/10.1016/j.compscitech.2018.08.046.
[30] D. Shahgholian-Ghahfarokhi, G. Rahimi, G. Liaghat, R. Degenhardt, F. Franzoni, Buckling prediction of composite lattice sandwich cylinders (CLSC) through the vibration correlation technique (VCT): Numerical assessment with experimental and analytical verification, Composites B 199 (2020) 108252, http://dx.doi.org/10.1016/j.compositesb.2020.108252.
[31] E. Skukis, G. Jekabsons, J. Andersons, O. Ozolins, E. Labans, K. Kalnins, Robustness of empirical vibration correlation techniques for predicting the instability of unstiffened cylindrical composite shells in axial compression, Polymers 12 (2020) http://dx.doi.org/10.3390/polym12123069.
[32] K. Kalniņš, E. Skuķis, O. Ozoliņš, G. Jēkabsons, VCT Vibration correlation technique for assessment of structural load bearing capacity. [Online] Insitute of Material and Technology Riga Technical Univrsity. [Cited:] http://vct.rtu.lv/results.html.
[33] M.A. Souza, Relevant Dynamic Effects in the Design of Thinwalled Structures, Vol. 49, IABSE reports, 1986, http://dx.doi.org/10.5169/seals-38291.
[34] M.A. Souza, The effects of initial imperfection and changing support conditions on the vibration of structural elements liable to buckling, Thin-Walled Struct. 5 (1987) 411–423, http://dx.doi.org/10.1016/0263-8231(87)90031-0.
[35] M.A. Arbelo, S. Castro, R. Khakimova, R. Degenhardt, Improving the correlation of finite element models using vibration correlation technique on composite cylindrical shells, in: Tel-Aviv and Haifa: 54th Israel Annual Conference on Aerospace Sciences, Vol. 1, 2014, pp. 453–459.
[36] A. Gliszczyński, F. Franzoni, T.D. Baciu, R. Degenhardt, Predictive capabilities of vibration-correlation technique applied to axially compressed CFRP truncated cones, Composites B 240 (2022) http://dx.doi.org/10.1016/j.compositesb.2022.109984.

[37] A. Segall, G.S. Springer, A dynamic method for measuring the critical loads of elastic flat plates, Exp. Mech. 26 (1986) 354–359, http://dx.doi.org/10.1007/BF02320151.

[38] C.G. Go, Y.S. Lin, E.H. Khor, Experimental determination of the buckling load of a straight structural member by using dynamic parameters. 3, J. Sound Vib. 205 (3) (1997) 257–264, http://dx.doi.org/10.1006/jsvi.1995.1047.

[39] T.D. Baciu, R. Degenhardt, F. Franzoni, K. Kalnins, A. Gliszczynski, M.A. Arbelo, S.G.P. Castro, Sensitivity to measurement parameters of the vibration correlation technique to predict shell buckling loads - a numerical study, in: European Conference on Spacecraft Structures, Materials and Environmental Testing (ECSSMET 2021), 2021.

[40] R. Degenhardt, A. Kling, A. Bethge, J. Orf, L. Kärger, R. Zimmermann, Investigations on imperfection sensitivity and deduction of improved knock-down factors for unstiffened CFRP cylindrical shells, Compos. Struct. 92 (8) (2010) 1939–1946, http://dx.doi.org/10.1016/j.compstruct.2009.12.014.

[41] F. Franzoni, M.A. Arbelo, R. Degenhardt, Numerical assessment of existing vibration correlation techniques, in: European Conference on Spacecraft Structures, Materials and Environmental Testing, ECSSMET, 2018, https://elib.dlr.de/124717/.

[42] S.G.P. Castro, R. Zimmermann, M.A. Arbelo, R. Khakimova, M.W. Hilburger, R. Degenhardt, Geometric imperfections and lower-bound methods used to calculate knock-down factors for axially compressed composite cylindrical shells, Thin-Walled Struct. 74 (2014) 118–132, http://dx.doi.org/10.1016/j.tws.2013.08.011.

[43] M. Glantz, R. Kissell, Multi-Asset Risk Modeling: Techniques for a Global Economy in an Electronic and Algorithmic Trading Era, Academic Press, 2014.

[44] P. Schober, C. Boer, L. Schwarte, Correlation coefficients: Appropriate use and interpretation, Anesth. Analg. 126 (5) (2018) 1763–1768, http://dx.doi.org/10.1213/ANE.0000000000002864.

[45] M.T. Puth, M. Neuhäuser, G.D. Ruxton, Effective use of spearman's and Kendall's correlation coefficients for association between two measured traits, Anim. Behav. 102 (2015) 77–84, http://dx.doi.org/10.1016/j.anbehav.2015.01.010.

[46] E.R. Botsch, Chapter 12. Significance and measures of association, 2011, http://polisci.usca.edu/apls301/Text/Chapter%2012.%20Significance%20and%20Measures%20of%20Association.htm.

[47] G.R. van den Berg, Kendall's tau – simple introduction. spss-tutorials, 2021, [Online] [Cited: 21 08 2021.] https://www.spss-tutorials.com/kendalls-tau/.